Sub-diffraction-limit imaging using mode multiplexing

Nan Wang[ab], Jinping He[ab], Jun Miyazaki[ab], Hiromichi Tsurui[c], Takayoshi Kobayashi[*abde]
[a] Advanced Ultrafast Laser Research Center, University of Electro-Communications, 1-5-1 Chofugaoka, Chofu, Tokyo 182-8585, Japan; [b]JST, CREST, 5 Sanbancho, Chiyoda-ku, Tokyo 102-0075, Japan; [c]Department of Pathology, School of Medicine, Juntendo University, 2-1-1, Hongo, Bunkyo-ku, Tokyo 113-8421, Japan; [d]Department of Electrophysics, National Chiao-Tung University, 1001 Ta Hsinchu Rd., Hsinchu 300, Taiwan; [e]Insitute of Laser Engineering, Osaka University, 2-6 Yamada-oka, Suita, Osaka 565-0971, Japan

ABSTRACT

Simultaneous two-color subtraction microscopy using mode multiplexing is realized experimentally. The samples are irradiated with single laser diode at wavelength of 445 nm. Then the beam split laser spots generate separate solid and donut spatial modes and are multiplexed with modulators for simultaneous excitation. The produced fluorescence signals are back collected and further divided into two color bands with dichroic mirrors. Then they are detected with two photomultipliers and demultiplexed in four lock-in amplifiers. Four fluorescence images are recorded in every scan and resolution enhanced images are obtained in two color channels after applying the subtraction strategy. With this method, imaging results of microspheres stained with organic dyes and mesenteric lymph nodes of a mouse labeled with quantum dots (Q525/650) are realized. Improvement of 20% ~ 30% in resolving power of the two color channels compared with confocal microscopy is achieved in with corresponding subtraction factor of about 0.3.

Keywords: subtraction microscopy, multicolor imaging, quantum dot, mode multiplexing, fluorescence imaging.

1. INTRODUCTION

To investigate nanoscale interaction or colocalization in biological tissues and microstructure materials, multi-color superresolution far field optical microscopy could be a powerful tool [1-3]. However the microscopes and fluorophores staining in the sample presently used to approach this goal still have some limitations. Firstly, optical superresolution microscopes, which have achieved great success in break the diffraction-limit, like simulated emission depletion microscopy (STED) [4], structured illumination microscopy (SIM) [5], photoactive localization microscopy (PALM) [6], stochastic optical reconstruction microscopy (STORM) [7], super-resolution optical fluctuation imaging microscopy (SOFI) [8], and others [9-13], are expensive and inflexible to build and maintain. Especially when they are applied for multi-color imaging, the schemes become quite costly and complicated [14-19]. Secondly, organic dyes, which have been widely used as fluorescent labels in multi-color imaging for decades, introduce inevitable fluorescence crosstalk due to their broadband emission spectra and are easily photobleached. In comparison, quantum dots (Qdots), which have narrowband fluorescence spectra that can be easily separated by mirrors, broadband absorption spectra that can be possibly excited by only single laser wavelength and are highly photochemistry stable [20, 21], have not been used in muliti-color superresolution microscopes, like in the popular STED, PALM or STORM, due to the special requirements of probes. Meanwhile, multi-color imaging by using SOFI or SIM with Qdots could be but has not been reported yet as far as we know, possibly due to the complexity of the schemes. Therefore, superresolution microscopes with simple method as well as generalized fluorescent probes would be preferred for multi-color superresolution imaging. Recently, fluorescence microscopy based on mathematical calibration of images obtained by different excitation spots to improve the point spread function (PSF) [22-25], provides an easier concept to realize sub-diffraction-limit imaging, such as fluorescence emission difference microscopy (FED) [22] and switching laser mode microscopy (SLAM) [23]. By measuring and subtracting two confocal images excited by a Gaussian-shape spot and a donut-shape spot, the resolution can be enhanced better than 25% compared with confocal microscopes. And with these methods, an extended library of fluorescent emitters, such as Qdots, can be used as multi-color labels. In between these methods, mode multiplexed subtraction microscopy [25] is able to achieve the measuring and image processing pixel by pixel by using simultaneous detection techniques, so it can inhabit errors due to mechanical drifts and image organism diffusion in live cells. Besides this potential, mode multiplexed subtraction microscope can also be possibly extended for multi-color imaging and

Scanning Microscopies 2015, edited by Michael T. Postek, Dale E. Newbury, S. Frank Platek, Tim K. Maugel,
Proc. of SPIE Vol. 9636, 96360A · © 2015 SPIE · CCC code: 0277-786X/15/$18 · doi: 10.1117/12.2186137

nonlinear harmonic imaging easily. In this paper, two-color fluorescence subtraction imaging is demonstrated. With a home-made mode multiplexed subtraction microscope, imaging of fluorescent beads stained with organic dyes and mesenteric lymph nodes labeled with Qdots is achieved. Resolution enhancement in both of the two color channels is obtained compared with confocal microscopes. By using commercially off the shelf laser diodes and lock-in detection, the cost of the imaging system can also be reduced and the signal-noise ratio (SNR) of it can be improved.

2. EXPERIMENTS AND RESULTS

2.1 Experimental setup

The layout of the imaging system is shown in Figure 1. The excitation laser source is a continuous wave laser diode (NICHIA) emitting light at wavelength of 445 nm. After the beam splitter, the two excitation beams are spatial filtered with polarization maintained single-mode fibers and phase filtered to have Gaussian and donut intensity distributions. For generating the donut spot, a vortex phase plate (RPC Photonics) is used to modulate the phase of the laser spot. Then the two beams are combined with a polarization beam splitter to have perpendicular polarizations in avoid of interference and focused into the sample by using an oil immersion objective lens (UPlanFLN100X/1.3, Olympus). The back reflected fluorescence is collected with the same objective and half amount of it is reflected for detection with a 50:50 beam splitter. Then the fluorescence passes through a long pass filter (LP03-458RU-25, Semrock) and split into two wavelength bands with a dichotic mirror (DMLP567, Thorlabs). The short wavelength component is reflected, further filtered by using a short pass filter (FES0600, Thorlabs) and detected with a voltage type photomultiplier (PMT). The electronic signals from this PMT are demultiplexed in two lock-in amplifiers (7270, Signal recovery) (LIA) as channel one (CH 1).The transmitted light component from the dichroic mirror has longer wavelength. It is detected with a current type photomultiplier (H11460, Hamamatsu), a current-voltage converter (C9999) and another two LIAs (7265, Signal recovery) as channel two (CH 2). Two chopper blades are installed to modulate the excitation beam paths; they encode the signals and then the trigger outputs of the chopper controllers (MC2000, Thorlabs) are sent to the reference inputs of the two LIAs. The modulation frequency of the Gaussian spot beam path (GBP) and donut shape beam path (DBP) is 4 kHz and 5 kHz, respectively. The sample is fixed on a three-axis piezoelectric controlled stage (MAX311D/M, Thorlabs) with a minimum scanning step of 5 nm using a closed-loop feedback drive (BPC303, Thorlabs). During the scan, the analog digital signal converter (LPC-361416, Interface, Japan) delivers the signal for stage control and acquire the fluorescence signals from the four LIAs simultaneously.

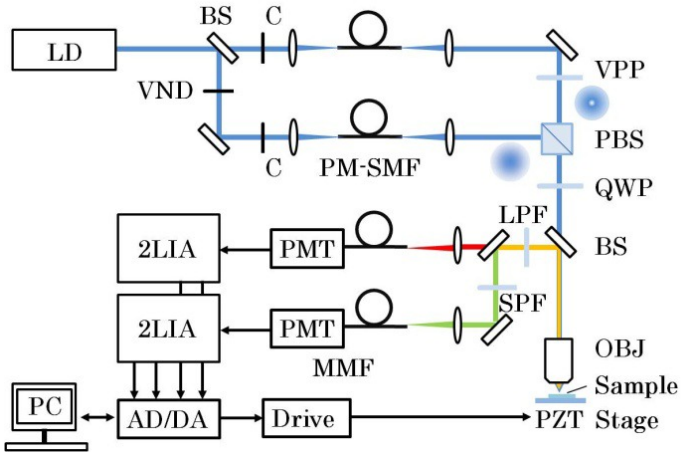

Figure 1. Experimental layout of the two-color subtraction microscopy. LD: laser diode; BS, beam splitter; VND, variable neutral density filter; PM-SMF, polarization maintained single mode fiber; C, Chopper; VPP, vortex phase plate; PBS, polarization beam splitter; QWP, quarter wave plate; OBJ, objective lens; MMF, multi-mode fiber; LPF, long pass filter; PMT, photomultiplier; LIA, lock-in amplifier; AD/DA: analog digital signal converter; PC, personal computer.

2.2 Samples

The fluorescent beads (T14792, life technologies) used for checking the imaging system are stained with four dyes. Since the excitation laser wavelength is out of absorption spectra of TetraSpeck blue, the fluorescence is emitted from the dye molecules of TetraSpeck green, orange, and dark red, absorption (dotted lines) and emission (solid lines) spectra

of which are shown in Figure 2(a). From the spectra, it can be seen the cross talk problem is serious in the two color channels while the dichroic mirror has the critical wavelength of 567 nm for separating the fluorescence. We found that, in our experiments the TetraSpeck green makes main contribution to the fluorescence in shorter wavelength channel while the emission from TetraSpeck orange and dark red perform an important role in the longer wavelength channel. It is difficult to completely separate the fluorescence of them, so presently the images obtained from CH2 include the fluorescence from the two dyes without being separated from each other via mathematical treatment. The biological sample is mesenteric lymph nodes of a mouse stained with Qdot525 for antibody CD8 (T cell) and Qdot650 for antibody B220 (B cell) (eFluo 525 NC / eFluo 650 NC, ebioscience), the excitation and fluorescence spectra of which are shown in Figure 2(b). From the spectra, it can be seen that the laser wavelength at 445 nm can excite both of them efficiently and the emitted fluorescence is able to be separated by the dichroic mirror. We checked the fluorescence spectra of two channels with a spectrometer (USB2000+, Ocean Optics) and found they agree with our prediction.

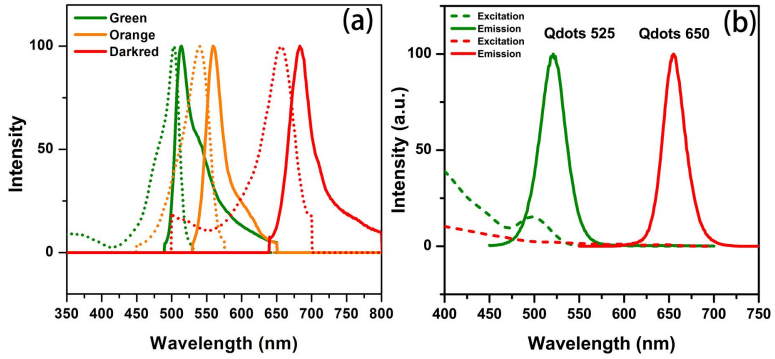

Figure 2. Absorption (dotted lines) and emission (solid lines) spectra of (a) fluorescent beads and (b) quantum dots.

2.3 Data processing

In the experiment, four confocal images are obtained in one scan period. Each of the color channels has two images demultiplexed from the LIAs, corresponding to the raw images from the excitation beams of GBP and DBP, respectively. To get the target image with improved resolution, the image of DBP is subtracted from the image of DBP with a factor. With a threshold subtraction factor [26], an appropriate resolution can be obtained to resolve the underlying feature of the sample without being over processed. However, a higher SNR is required for the imaging to inspect if the subtraction threshold reached or not via checking the peak intensity down to 0.6 of the initial value. In this experiment, the processing is performed in a simply and conservative way, $I_{Targ}=I_G(P, \lambda, h_{GT}, \eta_e)-I_D(P, \lambda, h_{DT}, \eta_e)$, where I_G and I_D are the individual images excited by GBP and DBP; P is the excitation power; λ is excitation wavelength; h_{GT} and h_{DT} are corresponding PSFs; η_e is detection efficiency. As was demonstrated experimentally [25], when the same excitation power of two beams are used, the peak to peak ratio of PSF of GBP and DBP is around 1:0.3. It means that, when the power of the two excitations beam is the same, the factor used for subtracting the two raw images is about 0.3. It is possible to enhance the resolution by increasing the weight of DBP, but the possibility of over-subtraction also increases. To avoid information loss of structures due to over subtraction, conservative direct subtraction here is implemented. Threshold subtraction is hopeful to be used when higher SNR images are obtained.

2.4 Experimental results

Firstly, fluorescent beads with radius of 100 nm are imaged. The results are shown in Figure 3. The excitation power of the GBP and DBP are both 4.86 μW. The dwell times and the time constants of all four LIAs are set to be 10 ms and 5 ms, respectively. The scanning step size is 20 nm and the scanning scale is 2 μm. With simultaneous measurement, four confocal images excited by GBP and DBP can be obtained and processed pixel by pixel in real time. The two-color confocal images excited by GBP are shown in Figures 3(a) and 3(b) while the overlapped image of them is displayed in Figure 3(c). The confocal images excited by GBP and DBP of CH1 are shown in Figure 3(i), corresponding to the PSF overlap of the two beams while similar images of CH2 would not be displayed. It can be seen that the confocal overlaps of the two color channels and the two PSFs are in good alignment. By directly subtracting the images excited by GBP and DBP, resolution enhanced images can be obtained, as are shown in Figures 3(d) and 3(e) while the overlap of them

is shown in Figure 3(f), indicating better resolution for colocalization of the two probes compared with confocal one shown in Figure 3(c). The cross sectioning lines in between head-faced white arrows in Figures 3(a), 3(d) and 3(b), 3(e) are shown in Figures 3(g) and 3(h), respectively. The values of full width at half maximum (FWHM) of the sectioning lines for subtracted images are about 180 nm and 160 nm. Compared with confocal resolution of 220 nm, resolution enhancement about 18% ~ 27% of the two channels can be achieved. This resolution difference of the two channels is due to the slightly overlap misalignment in the axial direction.

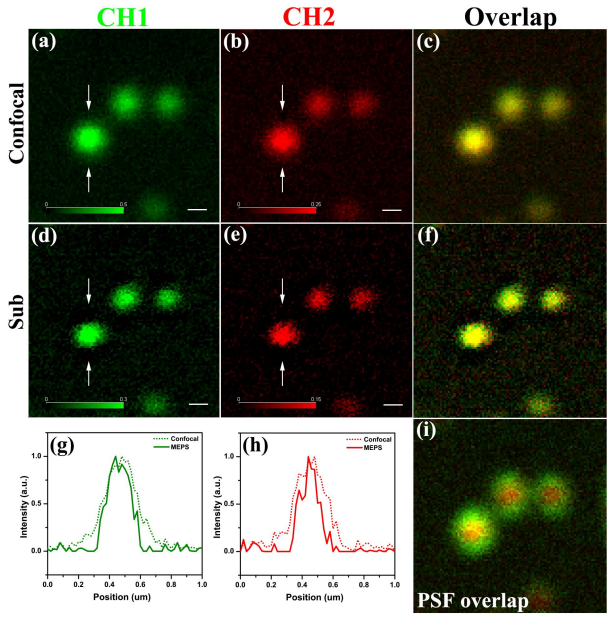

Figure 3. Two-color images of fluorescent beads in the range of 2 μm with mode multiplexed subtraction microscope. (a), (b) Two color confocal images and (c) their overlap, (d), (e) corresponding subtracted images and (f) their overlap. Overlap of (a) and donut confocal image is shown in (i). Sectioning lines between arrows in (a), (d) and (b), (e) are shown in (g) and (h) respectively. White scale bar: 200 nm.

The biological sample of mesenteric lymph nodes of a mouse labeled with Qdots 525/650 is imaged secondly. The excitation powers of GBP and DBP are measured to be 3.28 μW and 3.14 μW, respectively. The dwell time is 1 ms and time constants are set to be 500 μs for CH1 and 640 μs for CH2 because of the different model of lock-in amplifiers. The images of first column in Figures 4(a) gives simultaneous two-color images in scanning range of 20 μm with scale bar of 2 μm. The top one is the overlapped image while the middle and bottom ones are from CH1 and CH2, respectively. The zoomed confocal images in the area marked by the white squares are shown in the middle column of Figure 4(a). The scanning scale is 5 μm. With conjunction of antibodies B220 and CD8, the Qdots 525 and Qdots 650 would recognize immune B cells and T cells. However, because these cells are in scale of several micrometers, it is hard to check the fine colocalization in the experiment. Here, some isolated Qdots that have not been identically stained are used for imaging and could be observed. The subtracted images, as is shown in right column of Figures 4(a), are able to improve the resolution and SNR in comparison with the confocal imaging. And the two kinds of Qdots with tiny different distributions, pointed with the white arrow indicators, can be observed.

A second group of two-color images of the same biological sample at a different position is measured and are shown in Figure 4(b). The dwell time and time constant is set to be 10 ms and 5 ms, respectively. The laser and scanning parameters are the same with previous group. The left column of Figure 4(b) are simultaneous two-color images in scanning range of 20 μm with scale bar of 2 μm, while from top to bottom they are overlapped image of the two channels, images from CH1 and from CH2. The middle and right columns are the zoomed confocal images and corresponding subtracted images of the area marked by the white squares. The resolution is enhanced and the SNR of them are improved, as are shown in subtracted images.

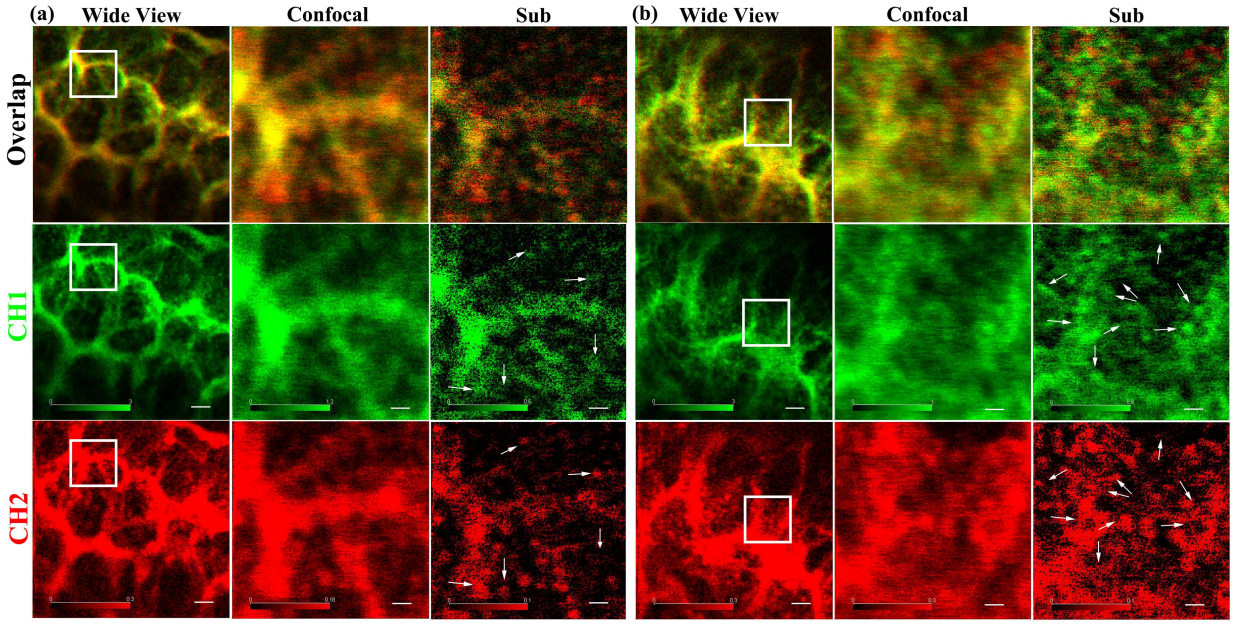

Figure 4. (a) and (b) are two groups of two-color imaging of mesenteric lymph nodes stained with Qdots 525/650. In each group, left columns are confocal images; middle columns are the confocal images of zoomed area marked with white squares in the wide view images; the right columns are the corresponding subtracted images. White scale bars in left columns: 2 μm; white scale bar in middle and right columns: 500 nm.

2.5 Discussion

With the excitation mode multiplexing and separate fluorescence detection, four fluorescence images are recorded at the same time and resolution enhancements in two wavelength bands can be realized simultaneously. One of the problems in present experiment is still the appropriate selection of the subtraction factor. In this paper, the same laser power of the two mode paths are used for excitation, corresponding to subtraction factor of 0.3. A larger subtraction factor is favorable to obtain a higher resolution. However, the possibility of over-subtraction also increases. In this case, it is better to check if the threshold subtraction is reached or not with peak intensity factor [26]. Due to the lower SNR in this two-color imaging, threshold subtraction is hopeful to be realized after further improvements are carried out. To promote the performance of present imaging system, optical and electrical parameters related to SNR are considered for optimization. On one hand, by replacing the current to voltage converter (Bandwidth: 10 MHz) of photomultiplier with a narrower bandwidth one, the noise level could be further suppressed. On the other hand, the beam splitter, which is used to separate back reflected fluorescence, gets a signal loss of 50% and will be changed with a dichroic mirror to improve the fluorescence collection efficiency. Although the single photon counting method has higher sensitivity for the fluorescence detection, the simultaneous data acquisition of the four channels is difficult to achieve and is highly cost. In the following, by staining the sample of fine structures with Qdots, colocalization of them would be able to be imaged with improved resolution. During the imaging process, photobleaching of fluorescent beads has been observed when the excitation power is higher than 5 μW for each beam. In comparison, the sample labeled with Qdots is more robust even when the excitation power exceeds this value. Qdots are demonstrated to be acting quite well in two-color subtraction imaging.

3. CONCLUSION

In conclusion, two-color fluorescence subtraction microscopy is experimentally demonstrated. Images of the fluorescent beads stained with organic dyes and the biological sample of mesenteric lymph nodes of a mouse labeled with quantum dots with improved resolution are obtained, corresponding to resolution enhancement of 20% ~ 30% compared with confocal microscopy when the same excitation power is implemented for the two excitation beams. With further improvement of scanning speed and signal noise ratio of the detection system, this microscopy is potential for multi-color sub-cellular colocalization and interaction analysis for live cells.

REFERENCES

[1] Neumann, D., Bückers, J., Kastrup, L., Hell, S. W. and Jakobs, S., "Two-color STED microscopy reveals different degrees of colocalization between hexokinase-I and the three human VDAC isoforms," PMC Biophy. 3(4) (2010)

[2] Friedemann, K., Turshatov, A., Landfester, K. and Crespy, D., "Characterization via Two-Color STED Microscopy of anostructured Materials Synthesized by Colloid Electrospinning," Langmuir 27, 7132-7139 (2011)

[3] Lakadamyali, M., Babcock, H., Bates, M., Zhuang, X. and Lichtman, J., "3D Multicolor Super-Resolution Imaging Offers Improved Accuracy in Neuron Tracing," PLOS 7, e30826 (2012)

[4] Hell, S. W. and Wichmann, J., "Breaking the diffraction resolution limit by stimulated emission: stimulated-emission-depletion fluorescence microscopy," Opt. Lett. 19, 780-782 (1994)

[5] Gustafsson, M. G. L., "Surpassing the lateral resolution limit by a factor of two using structured illumination microscopy," J. Microscopy 198, 82-87 (2000)

[6] Betzig, E., Patterson, G. H., Sougrat, R., Lindwasser, O. W., Olenych, S., Bonifacino, J. S., Davidson, M. W., Schwartz, J. L. and Hess, H. F., "Imaging Intracellular Fluorescent Proteins at Nanometer Resolution," Science 313, 1642-1645 (2006)

[7] Rust, M. J., Bates, M. and Zhuang, X. W., "Sub-diffraction-limit imaging by stochastic optical reconstruction microscopy (STORM)," Nat. Meth. 3, 793-796 (2006)

[8] Dertinger, T., Colyer, R., Iyer, G., Weiss, S. and Enderlein, J., "Fast, background-free, 3D super-resolution optical fluctuation imaging (SOFI)," P. Natl. Acad. Sci. USA 106, 22287-22292 (2009)

[9] Wang, Y., Fruhwirth, G., Cai, E., Ng, T. and Selvin, P. R., "3D Super-Resolution Imaging with Blinking Quantum Dots," Nano. Lett 13, 5233-5241 (2013)

[10] Gordon, M. P., Ha, T. and Selvin, P. R., "Single-molecule high-resolution imaging with photobleaching," P. Natl. Acad. Sci. USA 101, 6462-6465 (2004)

[11] Simonson, P. D., Rothenberg, E. and Selvin, P. R., "Single-Molecule-Based Super-Resolution Images in the Presence of Multiple Fluorophores," Nano Lett. 11, 5090-5096 (2011)

[12] Miyazaki, J., Tsurui, H., Hayashi-Takagi, A., Kasai, H. and Kobayashi, T., "Sub-diffraction resolution pump-probe microscopy with shot-noise limited sensitivity using laser diodes," Opt. Express 22(8), 9024-9032 (2014).

[13] He, J., Miyazaki, J., Wang, N., Tsurui, H. and Kobayashi, T., "Label-free imaging of melanoma with nonlinear photothermal microscopy," Opt. Lett. 40, 1141-1144 (2015)

[14] Rittweger, E., YoungHan, K., Irvine, S. E., Eggeling, C. and Hell, S. W., "STED microscopy reveals crystal colour centres with nanometric resolution," Nat. Photonics 3, 144-147 (2009)

[15] Donnert, G., Keller, J., Wurm, C. A., Rizzoli, S. O., Westphal, V., Schonle, A., Jahn, R., Jakobs, S., Eggeling, C. and Hell, S. W., "Two-Color Far-Field Fluorescence Nanoscopy," Biophys. J. 92, L67-L69 (2007)

[16] Gottfert, F., Wurm, C. A., Mueller, V., Berning, S., Cordes, V. C., Honigmann, A. and Hell, S. W., "Coaligned Dual-Channel STED Nanoscopy and Molecular Diffusion Analysis at 20 nm Resolution," Biophys. J. 105, L01-L03 (2013)

[17] Shroff, H., Galbraith, C. G., Galbraith, J. A., White, H., Gillette, J., Olenych, S., Davidson, M. W. and Betzig, E., "Dual-color superresolution imaging of genetically expressed probes within individual adhesion complexes," P. Natl. Acad. Sci. USA 104, 20308-20313 (2007)

[18] Bates, M., Huang, B., Dempsey, G. T. and Zhuang, X., "Multicolor Super-Resolution Imaging with Photo-Switchable Fluorescent Probes," Science 317, 1749-1753 (2007)

[19] Fiolka, R., Shao, L., Rego, E. H., Davidson, M. W. and Gustafsson, M. G. L., "Time-lapse two-color 3D imaging of live cells with doubled resolution using structured illumination," P. Natl. Acad. Sci. USA 109, 5311-5315 (2012)

[20] Bruchez, Jr. M., Moronne, M., Gin, P., Weiss, S. and Alivisatos, A. P., "Semiconductor Nanocrystals as Fluorescent Biological Labels," Science 281, 2013-2016 (1998)

[21] Jaiswal, J. K., Mattoussi, H., Mauro, J. M. and Simon, S. M., "Long-term multiple color imaging of live cells using quantum dot bioconjugates," Nat. Biotech 21, 47-51 (2003)

[22] Kuang, C. F., Li, S., Liu, W., Hao, X., Gu, Z. T., Wang, Y. F., Ge, J. H., Li, H. F. and Liu, X., "Breaking the Diffraction Barrier Using Fluorescence Emission Difference Microscopy," Sci. Rep. 3(1441) (2013)

[23] Dehez, H., Piché, M., and Koninck, Y. D., "Resolution and contrast enhancement in laser scanning microscopy using dark beam imaging," Opt. Express 21, 15912-15925 (2013)

[24] Segawa, S., Kozawa, Y. and Sato, S. "Resolution enhancement of confocal microscopy by subtraction method with vector beams," Opt. Lett. 39, 3118-3121 (2014)
[25] Wang, N., Miyazaki, J., He, J., Seto, K. and Kobayashi, T., "Sub-diffraction-limit imaging using mode multiplexing," Opt. Commun. 343, 28-33 (2014)
[26] Wang, N and Kobayashi, T, "Numerical study of the subtraction threshold for fluorescence difference microscopy," Opt. Express 22(23), 28819-28830 (2014)